



# Catalytic degradation of caffeine in aqueous solutions by cobalt-MCM41 activation of peroxymonosulfate

Fei Qi<sup>a,b</sup>, Wei Chu<sup>a,\*</sup>, Bingbing Xu<sup>c</sup>

<sup>a</sup> Department of Civil and Environmental Engineering, The Hong Kong Polytechnic University, Hung Hom, Kowloon, Hong Kong

<sup>b</sup> Beijing Key Lab for Source Control Technology of Water Pollution, College of Environmental Science and Engineering, Beijing Forestry University, Beijing 100083, PR China

<sup>c</sup> State Key Laboratory of Environmental Criteria and Risk Assessment, Chinese Research Academy of Environmental Sciences, Beijing 100012, PR China

## ARTICLE INFO

### Article history:

Received 22 November 2012

Received in revised form 21 January 2013

Accepted 22 January 2013

Available online 29 January 2013

### Keywords:

Co incorporated MCM41

Peroxydisulfate activation

Advanced oxidation process

Caffeine

Sulfate radicals

## ABSTRACT

In this study, the performance of caffeine degradation and mineralization in aqueous phase by a catalyst that was prepared by incorporating cobalt into the structure of MCM41 (i.e. Co-MCM41) in activating peroxymonosulfate (PMS) was explored. Experimental results showed that Co-MCM41 activated PMS not only degraded caffeine, but also mineralized the corresponding intermediates successfully. The surface and structure properties of Co-MCM41 were characterized by several analytical methods. The leaching of cobalt ions in this process was very low, and the heterogeneous reaction dominated the caffeine decay rather than the homogeneous one, which made the reuse of catalyst highly feasible. According to the result of using quenchers, both  $\text{OH}^\bullet$  and  $\text{SO}_4^{\bullet-}$  were found in this process and the latter was the major oxidant species. Furthermore, nine major intermediates generated in this process were identified and the degradation pathway was proposed.

© 2013 Elsevier B.V. All rights reserved.

## 1. Introduction

Pharmaceutical and personal care products (PPCPs) have received increased attention as aquatic contaminants due to the extensive use of antibiotics, mental drugs, hormone drugs, and musk from synthetic or natural sources [1]. The concentration of PPCPs in sewage treatment plant effluents [2], surface/ground water [3], lake water [4], and raw/source water is ranged from ng/L to  $\mu\text{g/L}$ . The presence of PPCPs in water will produce negative effects on the aquatic organism and ecological environment due to their resistance to natural degradation and potential toxicity to aquatic organism and human life [5]. Therefore, it is of interest to develop efficient water treatment method for removing PPCPs from aquatic environments.

Advanced oxidation processes (AOPs) are generally recognized as the most effective methods for the degradation of hazardous, refractory and non-biodegradable organic pollutants, because of the generation of active oxygen species [6]. AOPs can theoretically destroy the structure of chemicals and mineralize them to carbon dioxide and water. The typical AOPs involve in catalytic ozonation [7,8], photodegradation [9,10], ultraviolet irradiation [11,12] and Fenton's process [13]. In recent years, sulfate radical ( $\text{SO}_4^{\bullet-}$ ) based-advanced oxidation processes (SR-AOPs) have attracted attentions in the water industry [14]. In this process,  $\text{SO}_4^{\bullet-}$  is generated by

combining persulfate or peroxymonosulfate (PMS) with transition metals [15], catalysts [16], UV [17], or ultrasound [18]. Moreover,  $\text{SO}_4^{\bullet-}$  demonstrates higher standard reduction potential (2.5–3.1 V [19]) than hydroxyl radicals ( $\text{OH}^\bullet$ , 1.8–2.7 V [20]) at the neutral pH and is more selective in an oxidation process than hydroxyl radicals at acidic pH [21].

Several investigations reported that the combination of Co and PMS is a good method for organic degradation in wastewater treatment [22,23]. However, the use of non-recoverable cobalt ions in the treatment process raises a concern due to its toxicity. Developing an efficient heterogeneous catalytic reaction therefore is a worthwhile alternative to minimize the discharge of cobalt in the treated effluent. Several attempts have been made by using Co oxides [24], supported Co [25–27], and Co exchanged zeolites [28] as the heterogeneous catalysts for activating PMS. However, cobalt ion leaching was observed in different scales for various catalysts.

In this study, Co was incorporated into MCM41, a mesoporous silica with hexagonal order pore canal (named as Co-MCM41) and used as the heterogeneous catalyst for PMS activation. The incorporation of cobalt into the structure of MCM41 could immobilize cobalt ion and eventually minimize the metal leaching. Caffeine (CAF) was selected as the probe in this study. CAF is the most commonly used legal drug throughout the world, whether in the form of beverages or combined with analgesics to enhance its effect [29]. CAF is readily metabolized by human; the disposal of the unconsumed coffee and soft drinks is the predominant source of CAF introduced into the wastewater stream [30]. Furthermore, it was also used as a chemical marker for

\* Corresponding author. Tel.: +852 2766 6075; fax: +852 2334 6389.

E-mail address: [cewchu@polyu.edu.hk](mailto:cewchu@polyu.edu.hk) (W. Chu).

surface water pollution caused by municipal wastewater, since the human species almost exclusively consumes and excretes it or its metabolism regularly [30]. In this investigation, the physicochemical properties of catalyst were characterized, and the performance of the combination of Co-MCM41 and PMS in degradation CAF was evaluated. The intermediates generated in this process were identified, and the degradation pathway was proposed.

## 2. Materials and methods

### 2.1. Chemicals and reagents

All chemicals were of analytic reagent grade and all solvents were of high performance liquid chromatography (HPLC) grade; they were used as received without any further purification. Oxone (95%) was purchased from Sigma–Aldrich Inc. (USA), while caffeine (99%) was purchased from International Laboratory (USA). Distilled-deionized water with a resistivity of 18.2 MΩ cm generated from a Bamstead NANO pure water treatment system (Thermo Fisher Scientific Inc., USA) was used to prepare all the solutions. Nitric acid and/or sodium hydroxide were used to adjust the initial pH of the solution. To prepared MCM41 or Co-MCM41, the tetraethylorthosilicate (TEOS, 98% GC) and hexadecyl trimethyl ammonium bromide (CTAB) were purchased from Sigma–Aldrich Inc. (USA).

### 2.2. Synthesis of Co-MCM41 catalysts

The synthesis of Co-MCM41 followed the procedure described by De Souza et al. [31]. In a typical synthesis procedure, 2.4 g CTAB was dissolved in 120 g de-ionized water by ultrasonic wave. After adding  $\text{Co}(\text{NO}_3)_2 \cdot 6\text{H}_2\text{O}$  (0.0008 mol) into the above clear solution, aqueous ammonia solution (10.5 mL, 25 m/m%) was added and stirred for 15 min. Under stirring, TEOS (0.048 mol, 10.7 mL) was added drop-wise within a couple of minutes, then the gel started to form. The mixture was stirred for 2 h and aged for additional 16 h. After that, the precipitates were filtered and rinsed several times until a neutral pH was reached. The samples were then dried for 12 h at 333 K. Template removal was achieved by heating the samples in air up to 813 K at a heating rate of 2 K/min, followed by isothermal treatment at the same temperature for 6 h in air. In this MCM41 product, the ratio of Si and Co was fixed at 60. For MCM41 synthesis, no Co source was added.

### 2.3. Characterization of Co-MCM41 catalysts

The crystalline form of the catalysts was identified by X-ray diffractometer (XRD) on a Rigaku D/MAX-rA diffractometer (Japan) with a  $\text{Cu K}\alpha$  radiation at a scanning rate of  $2^\circ/\text{min}$ , and the samples were scanned at  $2\theta$  from  $1^\circ$  to  $90^\circ$ . The surface area and pore characterization of catalysts were determined by  $\text{N}_2$  adsorption–desorption at 77 K with a BRT-BJH Quantachrome (Model Nova 1200). The atomic composition of the MCM41 and Co-MCM41 was detected by X-ray photoelectron spectroscopy (XPS). The XPS spectrum was recorded on an Axis Ultra photoelectron spectrometer (Kratos Analytical Ltd., Japan) with  $\text{Al K}\alpha$  (1486.6 eV) as the X-ray source. All XPS spectra were corrected using the C 1s line at 284.6 eV. UV–vis diffuse reflectance spectroscopic (DRS) studies were carried out using a Lambda35 (Perkin Elmer, USA) equipped with an integrating sphere at the room temperature in air.  $\text{BaSO}_4$  was used as the reference material. All the spectra were recorded over the wavelength range from 240 to 800 nm.

### 2.4. Kinetic study of caffeine oxidation in Co-MCM41 activation PMS

The catalytic oxidation of CAF was carried out in a 500 mL reactor containing 0.05 mM CAF solution in room temperature. A known amount of oxidant, PMS from stock solution, was added to the mixture, then a known quantity of catalysts was added in the reactor to start the reaction. At the predetermined time interval, 10.0 mL sample was withdrawn using a syringe filter. For the determination of CAF and total organic carbon (TOC), the reaction was immediately quenched by  $\text{Na}_2\text{S}_2\text{O}_3$  solution (1.0 M), where 0.5 mL methanol solution was used as the quencher for the determination of the intermediates. The concentration of CAF was analyzed using a HPLC (from Waters Instrument, USA) with a UV detector at the wavelength of 273 nm with a Restek pinnacle octylamine (5  $\mu\text{m}$ , 0.46 cm  $\times$  25 cm) column. The mobile phase was 60%  $\text{CH}_3\text{CN}$  and 40% phosphoric acid solution (0.08%). Total Organic Carbon was determined by Total Organic Carbon Analyzer (TOC-5000A, Shimadzu). The identification of intermediates was conducted by a Finnigan SpectraSYSTEM<sup>®</sup> LC cooperated with a Thermo Quest Finnigan LCQ Duo mass spectrometer system which was equipped with an electrospray ionization interface operating at electrospray ionization mode (LC-ESI/MS). The effluent (0.8 mL/min) was delivered by a gradient system from a Thermo P4000 partitioned by the same column described before. The mobile phase was a mixture of 0.1% formic acid (A) and acetonitrile solution (B) containing 0.1% formic acid and 5% pure water, which was carried out according to the following gradient mode: (1) 95% of A was kept during the first 3 min; (2) from 3 to 53 min, B was linearly increased from 5 to 60%, while A was steadily decreased to 40%, then held for 2 min; and (3) from 55 to 59 min, the mobile phase was returned to the initial composition until the end of the run.

After the reaction, the spent catalysts were recovered from the reaction mixture by filtration (0.45  $\mu\text{m}$ ), washed thoroughly with distilled water overnight, and dried at  $70^\circ\text{C}$  for reuse.

The concentration of PMS stock solution and the remaining of PMS during the reaction were analyzed by an iodometric method [32]. The dissolution of cobalt ion during the reaction was analyzed by a spectroscopic methodology [14].

## 3. Results and discussion

### 3.1. Characterization of Co-MCM41 catalysts

The low-angle XRD diffraction patterns of the MCM41 and Co-MCM41 with different ratios of Si and Co synthesized at the room temperature are shown in Fig. 1. All samples exhibited a strong (1 0 0) diffraction peak at  $2\theta$  of  $2.2^\circ$ , and two lower intensities 110 and 200 at  $2\theta$  of  $3.8^\circ$  and  $4.4^\circ$ , respectively. These results indicated that MCM41 structure was retained after the direct introduction of cobalt into its framework [33]. The introduction of cobalt in MCM41 also led to the decrease of its diffraction peak intensities, which indicated a relatively disordered mesoporous structure arising from the introduction of cobalt. In addition, as seen from the inset, no diffraction peaks of cobalt oxide crystal appeared in the wide-angle XRD pattern of Co-MCM41, suggesting cobalt was incorporated into the framework position and/or walls of MCM41 mesoporous molecular sieve [34].

The  $\text{N}_2$  adsorption/desorption isotherms of MCM41 and Co-MCM-41 samples are shown in Fig. 2. All the samples provided the type IV isotherm of mesoporous materials with a sharp ramp in the relative pressure range of 0.25–0.40, which is due to the capillary condensation of nitrogen in the pores [35]. The pore diameter, pore volume and surface area of MCM41 and Co-MCM41 samples are presented in Table 1. Results showed that its surface area decreased

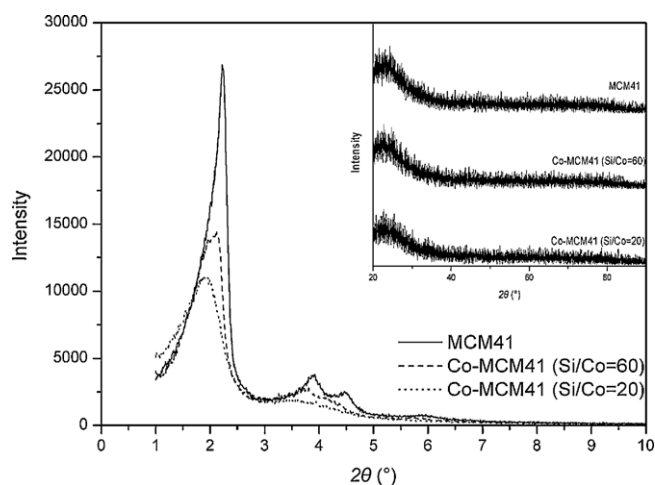


Fig. 1. XRD patterns of Co-MCM41 catalyst.

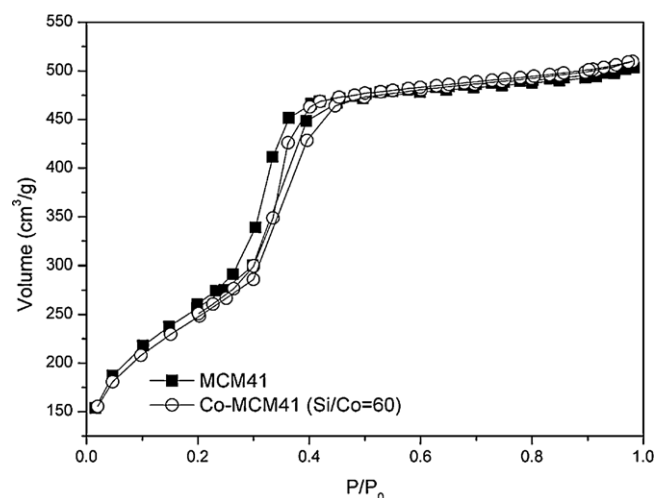


Fig. 2. N<sub>2</sub> adsorption isotherm and pore size distribution of Co-MCM41 catalyst.

when a certain amount of cobalt was introduced into the framework of MCM41, while the pore volume and size increased. These are attributed to the existence of cobalt species in the channels. A similar result about incorporation of other metals (such as Co, La, and Rh) into the silicate framework was reported [36]. Table 1 also shows MCM41 sample has an average pore diameter of 3.35 nm, Co-MCM41 exhibits slightly wider pore size distribution (average pore diameter 3.53 nm) than that of MCM41. Results suggest that Co-MCM41 retains the uniform mesoporous structure as MCM41.

Fig. 3 shows XPS results of MCM41 and Co-MCM41 samples. The XPS technique was used to determine the state of Co species in the prepared samples. For MCM41, there was no peak detected in the binding energy (BE) range. According to the XPS results and deconvolution analysis, there are 6 peaks for different cobalt species in Co-MCM41. The peaks at 782.1 (peak 5) and 797.5 eV (peak 2) are resulted from a chemical shift of the main spin-orbit components, because the Co cation on the nanocrystal surface is chemically

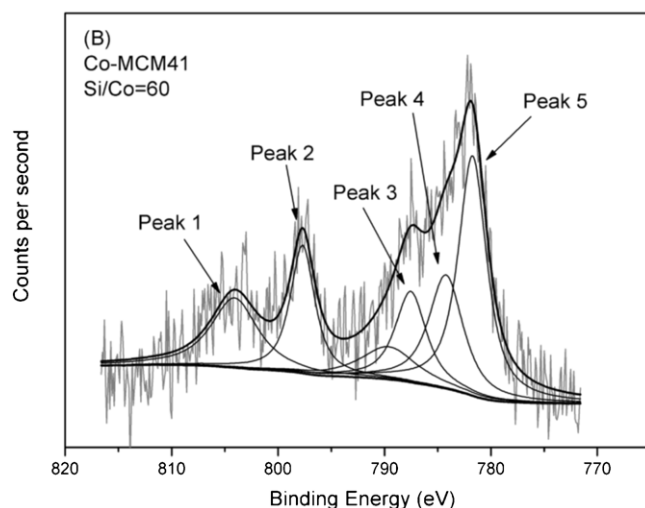
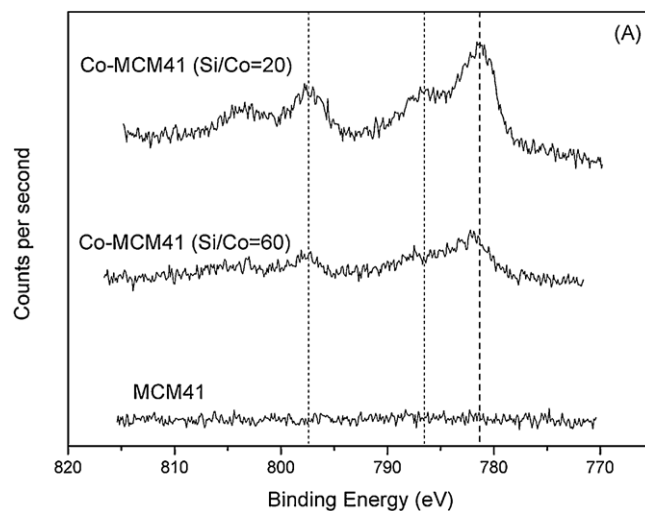


Fig. 3. XPS spectra of Co-MCM41 catalyst and Co species on the surface, (A) Surface of Co-MCM41 and MCM41; (B) identification of cobalt species on Co-MCM41.

interacted with surface hydroxyl ( $-\text{OH}$ ) or  $\text{Si}-\text{O}(-\text{OH}^*)$  or  $\text{Si}-\text{O}$  [37]. The corresponding shake-up satellite peaks for them are centered at 786.9 eV (peak 4) [37,38], as the BE of cobalt in  $\text{Co}_3\text{O}_4$  is normally at 780.4 eV (peak 6) for Co 2p<sub>3/2</sub> in the sample [38]. Shake-up satellites centered at 789.0 (peak 3) and 805.8 eV (peak 1) are also the characteristics of the  $\text{Co}_3\text{O}_4$  [39]. The presence of  $\text{Co}_3\text{O}_4$  is likely due to the Co species that are not incorporated into the structure of MCM41.

Fig. 4 shows UV–vis diffuse reflectance spectra (DRS) of MCM41 and Co-MCM41. For MCM41, there was no significant peak in the profile. In general, two broad peaks at 434 and 740 nm are due to the formation of  $\text{Co}_3\text{O}_4$ , where a migration of  $\text{Co}^{3+}$  ions to octahedral position occurs [40]. In this study, these two peaks were not observed in Co-MCM41 for two different Si/Co ratios at 20 and 60. It indicated that the content of  $\text{Co}_3\text{O}_4$  on the surface of Co-MCM41 is insignificant. Four major peaks were observed centered at 240, 530, 590, and 640 nm. For peaks at 240 and 530 nm, they confirm the presence of  $\text{Co}(\text{H}_2\text{O}_6)^{2+}$ ; for peaks at 590 and 640 nm, they suggest the existence of  $\text{Co}^{2+}$  in the crystal cell [14,28]. These peaks in Co-MCM41 indicate the existence of  $\text{Co}^{2+}$  in the mesoporous structure. As the cobalt content in MCM41 increased, the absorbance increased, suggesting more cobalt is incorporated into the structure of MCM41.

Table 1

Surface area and pore characteristics of Co-MCM41 prepared from different ratio of Si and Co.

Catalyst	Surface area (BET, $\text{m}^2/\text{g}$ )	Pore volume ( $\text{mL/g}$ )	Average pore diameter (nm)
MCM41	929.626	0.7783	3.35
Co-MCM41 (60)	894.883	0.7887	3.53

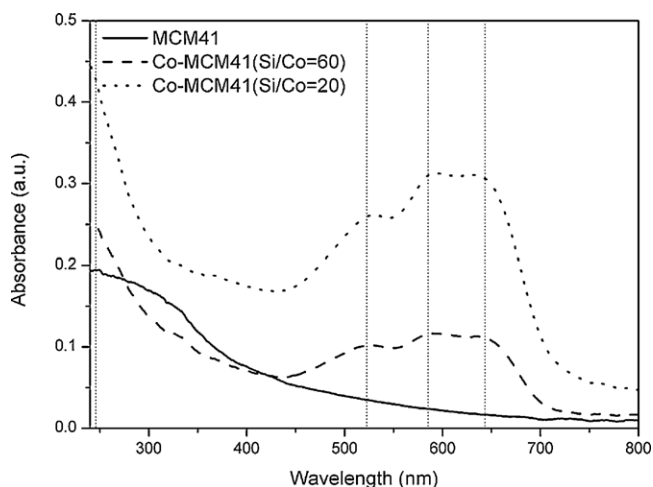


Fig. 4. UV-vis diffusive reflectance spectra of Co-MCM41 catalyst.

### 3.2. Performance and mineralization of Co-MCM41 activated PMS for caffeine degradation

The CAF degradation profiles in the processes of MCM41 and Co-MCM41 (Si/Co = 60) are shown in Fig. 5 and the ratio of PMS/CAF is 4.0. For comparison, catalysts such as cobalt ion ( $\text{Co}^{2+}$ ), CoO solid, and cobalt supported (non-incorporated) on MCM41 (defined as Co/MCM41, Si/Co = 60) were also investigated. For the oxidation of CAF by PMS alone, the reaction was insignificant, indicating catalyst is surely required in activating PMS for CAF degradation. MCM41 itself did not activate PMS since there is no active metal or metal oxide in it (mainly silicon). In contrast, a relatively fast CAF degradation kinetics was achieved in the Co-MCM41 activated PMS process, where CAF was completely degraded in 20 min.

From the previous study, both CoO [24] and  $\text{Co}_3\text{O}_4$  [41,42] were reported to activate PMS for the degradation of organic pollutants. Two typical dosages of CoO were applied to simulate the heterogeneous process. One was by using 200 mg/L CoO ( $\nabla$ ), the same mass as Co-MCM41 for general comparison; the other was the use of 0.597  $\mu\text{M}$  (35.22  $\mu\text{g/L}$ ) CoO ( $\nabla$ ) and the cobalt was equivalent to the cobalt dosage used in making the Co-MCM41. In both cases, the removal efficiencies were lower than that of Co-MCM41. The

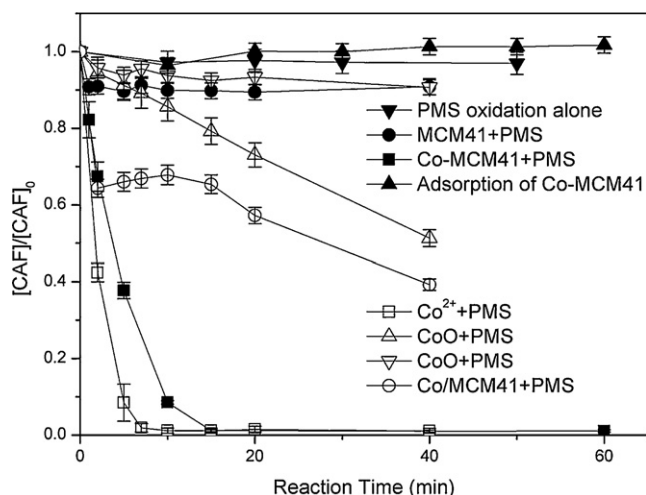


Fig. 5. Performance of Co-MCM41 activation PMS for caffeine degradation. Reaction condition: in all experiments  $[\text{CAF}]_0 = 0.05 \text{ mM}$ ,  $[\text{PMS}]_0 = 0.2 \text{ mM}$ , water pH was not controlled at 3.73; (●)  $[\text{MCM41}] = 200 \text{ mg/L}$ , (■)  $[\text{Co-MCM41}] = 200 \text{ mg/L}$ , (▲)  $[\text{Co-MCM41}] = 200 \text{ mg/L}$ , (○)  $[\text{Co/MCM41}] = 200 \text{ mg/L}$ , (□)  $[\text{Co}^{2+}] = 0.597 \text{ mM}$  (35.16  $\mu\text{g/L}$ ), (△)  $[\text{CoO}] = 200 \text{ mg/L}$ , and (▽)  $[\text{CoO}] = 0.597 \text{ mM}$  (44.73  $\mu\text{g/L}$ ).

former (higher dosage of CoO) had a higher removal efficiency, while for the latter (lower dosage), the removal efficiency was very low. This result indicates that equivalent cobalt dosage in Co-MCM41 led to higher catalytic activity. The incorporation of cobalt into the structure of MCM41 results in a higher utilization of cobalt in activating PMS. Furthermore, cobalt oxides were also supported on the surface of SBA-15 as another typical mesoporous [27],  $\text{TiO}_2$  [43],  $\text{SiO}_2$  [26],  $\text{MgO}$  [44] and red mud [45]. Their results suggested that the cobalt oxides on the supporting media are capable of activating PMS. In this study, the catalytic activity of cobalt oxide-supported MCM41 (Co/MCM41, Si/Co = 60, ○) was therefore studied, however, the catalytic activity of Co/MCM41 (supported Co) was much lower than that of Co-MCM41 (incorporated Co). The Co oxides, including CoO and  $\text{Co}_3\text{O}_4$ , are formed on the surface of MCM41 for the Co/MCM41. Although the CoO and  $\text{Co}_3\text{O}_4$  were reported to be effective heterogeneous catalysts for activating PMS, the incorporation of cobalt into the structure of MCM41 (Co-MCM41), however results in a higher removal efficiency than that by simply loading cobalt oxide on the surface of MCM41 (Co/MCM41).

To compare the performance between the homogeneous and heterogeneous reactions, cobalt ion as the activator of PMS in homogeneous phase for degradation CAF was also carried out. The dosage of cobalt ion ( $\square$ ) was equivalent to the cobalt content in Co-MCM41 (200 mg/L, Si/Co = 60). It is not surprised that cobalt ion achieves a higher removing efficiency than that of Co-MCM41, in which CAF was degraded completely in 10 min. However, the releasing of cobalt ions into the environment via an uncontrolled homogeneous process is a concern. The possible leaching of cobalt and its effect on activating PMS reaction therefore will be discussed in-depth later.

Several studies reported the removal efficiency of CAF by different oxidation processes, such as UV photolysis, Fenton, photo-Fenton and photocatalytic reaction. Javier Rivas reported that UV-C photolysis led to over 95% removal of CAF (0.12 mM) in 120 min reaction [46]. The oxidation capacity of UV photolysis was weaker. Álvarez et al. reported that in the presence of a magnetic  $\text{TiO}_2$  catalyst ( $\text{TiO}_2/\text{SiO}_2/\text{Fe}_3\text{O}_4$ , 1.34 g/L), over 95% CAF (0.154 mM) was photolysis in 240 min reaction [47]. Trovó et al. tried to optimize the photo-Fenton process and the residual CAF was lowered to its quantitation limit (0.004 mM) in 20 min reaction [48]. In addition, a solar photo-Fenton process could remove 95% CAF (0.1 mg/L) from the effluent of municipal wastewater in 40 min reaction [49]. In comparison, the Co-MCM41 activated PMS showed a promising performance in removing CAF.

To further evaluate the performance of Co-MCM41 activated PMS, mineralization capacity tests were carried out with different ratios of PMS and CAF basing on the concentration of CAF being 0.05 mM (Fig. 6). As describe above, the ratio of PMS/CAF at 4.0 achieved a good efficiency in degradation CAF (Fig. 5). There was no mineralization at all in 40 min, and only less than 10% of mineralization was observed after 100 min of reaction under this reaction condition. This is likely due to the deficiency of oxidants (i.e.  $\text{SO}_4^{\bullet-}$  or  $\text{OH}^{\bullet}$ ) in the solution, so the decay of CAF's daughter compounds was retarded. As the ratio of PMS/CAF increased to 40, a good mineralization (over 60% reduction of TOC) was achieved in 120 min. This justifies that sufficient oxidants is required if the treatment is targeted for a good mineralization.

### 3.3. Effect of Si/Co on the performance and cobalt leaching

Fig. 7 shows the leaching concentration of cobalt ions in PMS and Co-MCM41 with different Si/Co ratios. The increase of Si/Co ratio (i.e. the content of cobalt in the structure decreased) led to the decrease of CAF degradation rate. Such a reduction became more apparent for higher dosage of PMS (ratio of PMS/CAF = 4).

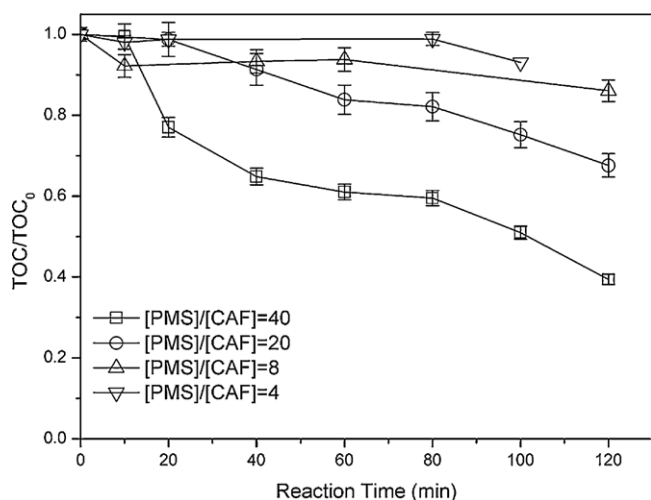


**Fig. 6.** Mineralization performance of Co-MCM41 activation PMS for caffeine degradation. Reaction condition:  $[CAF]_0 = 0.05$  mM,  $[catalyst] = 200$  mg/L, water pH was not controlled at 3.73.

This result also confirmed the leaching of cobalt ion in the process, where lower the Si/Co ratio, higher the leaching. However, the leaching of cobalt from Co-MCM41 was generally low ranging from only 2.57% to 3.9%. To evaluate the impact of cobalt leaching in the process, the equivalent dosages of cobalt ions were introduced to the reaction, and the result is shown in the inset of Fig. 7. It is interesting to note that the removal of CAF was insignificant under these circumstances. Therefore, the heterogeneous reaction between Co-MCM41 and PMS dominates the degradation of CAF.

#### 3.4. Effect of radical quenchers on the treatment performance

Activation of PMS with cobalt ions or cobalt-based catalyst mainly generates  $OH^\bullet$  and  $SO_4^{\bullet-}$  [50,51]. A minor peroxy-monosulphate radical ( $SO_5^{\bullet-}$ ) is also reported to be generated simultaneously, however its activity is very low compared with  $OH^\bullet$  or  $SO_4^{\bullet-}$ . To realize the type of active radicals present in the Co-MCM41 activated PMS process, a few quenching tests were carried out. Ethanol and *tert*-butyl alcohol (TBA) were used as quenching reagents with different concentrations. Ethanol is capable of quenching both  $SO_4^{\bullet-}$  ( $3.5 \times 10^7$  M $^{-1}$  s $^{-1}$ ) and  $OH^\bullet$

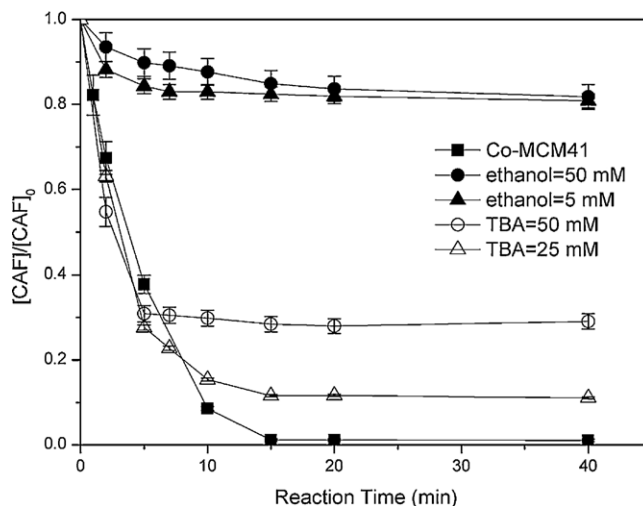


**Fig. 8.** Effect of radical quencher on performance of Co-MCM41 activation PMS. Reaction condition:  $[CAF]_0 = 0.05$  mM,  $[PMS]_0 = 0.2$  mM,  $[catalyst] = 200$  mg/L, water pH was at 7.10 with 0.1 M NaOH.

( $9.1 \times 10^6$  M $^{-1}$  s $^{-1}$ ) as it has a high reactivity toward both radicals [52], whereas TBA mainly reacts with  $OH^\bullet$  ( $3.8\text{--}7.6 \times 10^8$  M $^{-1}$  s $^{-1}$ ) and is less sensitive to  $SO_4^{\bullet-}$  ( $4.0\text{--}9.1 \times 10^5$  M $^{-1}$  s $^{-1}$ ) [52].

Fig. 8 shows the rate of CAF degradation in the presence of various quenching reagents. It was observed that the rate of reaction was significantly quenched at two different dosages of ethanol (100 or 1000 times of  $[CAF]$ ) with similar inhibiting effects. This indicated that the radicals generated in the system of Co-MCM41 in activating PMS were mostly quenched. The quenching effect of TBA on the process was much lower than that of ethanol. Only about 10% of inhibition (in terms of overall removal) was observed at 25 mM TBA (250 times of  $[CAF]$ ); and higher the TBA, higher the retardation. This result suggested that the dominant radical formed in the process is  $SO_4^{\bullet-}$ .

#### 3.5. Effect of reaction parameters on the performance

Fig. 9 presents the effect of PMS/CAF ratio on the oxidation process, where higher the ratio, better the CAF degradation rate and efficiency. The rate constant was found linearly increased with the ratios, as the ratio increased from 1 to 4, the rate

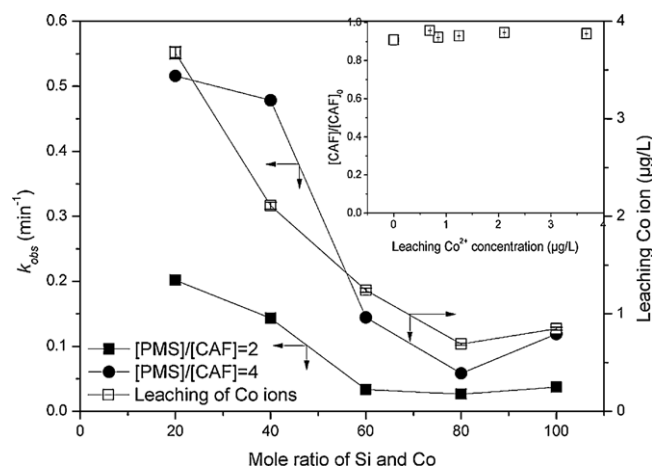


**Fig. 7.** Leaching of Co ion in heterogeneous reaction of different Co loading. Reaction condition:  $[CAF]_0 = 0.05$  mM,  $[catalyst] = 200$  mg/L, water pH was at 7.10 with 0.1 M NaOH.

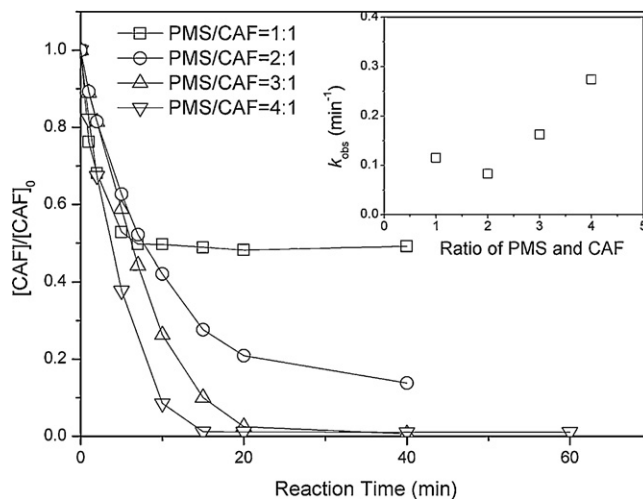


**Fig. 9.** Effect of ratios of PMS and caffeine on the performance. Reaction condition:  $[CAF]_0 = 0.05$  mM,  $[catalyst] = 200$  mg/L, water pH was not controlled at 3.73.

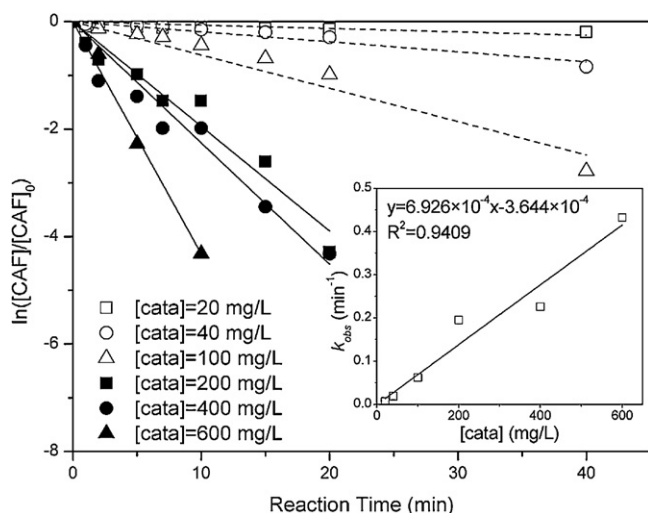


**Fig. 10.** Effect of Co-MCM41 mass on the performance. Reaction condition:  $[CAF]_0 = 0.05$  mM,  $[PMS]_0 = 0.2$  mM, water pH was not controlled at 3.73.

constant tripled. From the result of Fig. 6, it is expected that the increment of the PMS/CAF ratio would also lead to an improved mineralization, simultaneously. The higher PMS/CAF ratio generally provides more oxidants and therefore more radicals for the decomposition of intermediates.

Fig. 10 displays the CAF degradation by PMS at various Co-MCM41 catalyst dosages. Higher Co-MCM41 dose in solution resulted in higher CAF degradation rate and efficiency. The efficiency was clearly attributed to the increased number of active sites that can be used to generate more  $SO_4^{\bullet-}$ . Inset of Fig. 10 shows that the reaction rate increased with catalyst dosage and a linear relationship could be established between them.

### 3.6. Stability of Co-MCM41 in serial heterogeneous reaction

For the heterogeneous CAF oxidation by using Co-MCM41 and PMS, it is essential to examine the catalytic efficiency of the spent/reused catalyst. The catalyst was reused five times to examine its performance in oxidizing CAF and the results are shown in Fig. 11. As expected, there was a small reduction of the performance after each run, as noted from the slower initial decay rates. In practice, if a longer reaction time is adopted, a satisfactory removal efficiency of CAF can always be obtained after each run. The accumulation of intermediates from the previous run is likely the reason to cause this performance drop. The adsorbed intermediates were confirmed to remain on the catalyst surface and could not be fully removed by simple water rising. They will compete for the radicals with CAF coming from the next run.

### 3.7. Identification of intermediates and decay pathways of caffeine

To identify the degradation intermediates of CAF in the Co-MCM41/PMS process, the initial concentration of CAF was increased to 0.5 mM for a better resolution. The transformation of CAF and the formation and/or destruction of intermediates were monitored by LC-ESI/MS analysis. Such measurements permitted elemental compositions to be proposed for the protonated or sodiated adducts of the detected compounds as well as of their characteristic products ions. Totally, 9 intermediates were identified in this process, in which the compounds C1, C2 and C6 have never been reported before. The molecular weight, and structural formula of the identified intermediates are summarized in Table S1, and the ESI/MS of each compound is shown in Fig. S1. The compound marked as C9 with a deprotonated form ( $m/z$  at 225) is corresponding to a mass 32 Da with respect to the deprotonate CAF. This compound is likely the hydroxylated form of the 1,3,7-trimethyluric acid, as also reported by Telo et al., as an intermediates of radical oxidation [53], which contains two additional

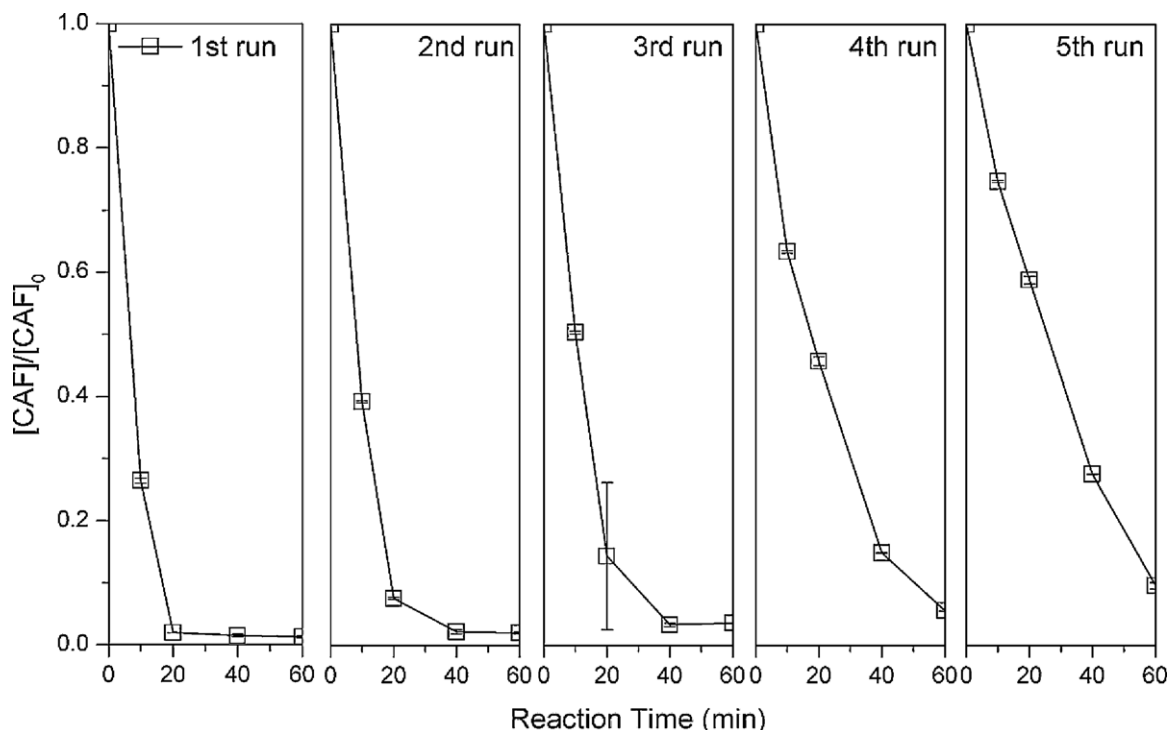


**Fig. 11.** Degradation of caffeine in consecutive runs using the recycled Co-MCM41. Reaction condition:  $[CAF]_0 = 0.05$  mM,  $[PMS]_0 = 0.2$  mM [catalyst] = 200 mg/L, water pH was at 7.10 with 0.1 M NaOH.

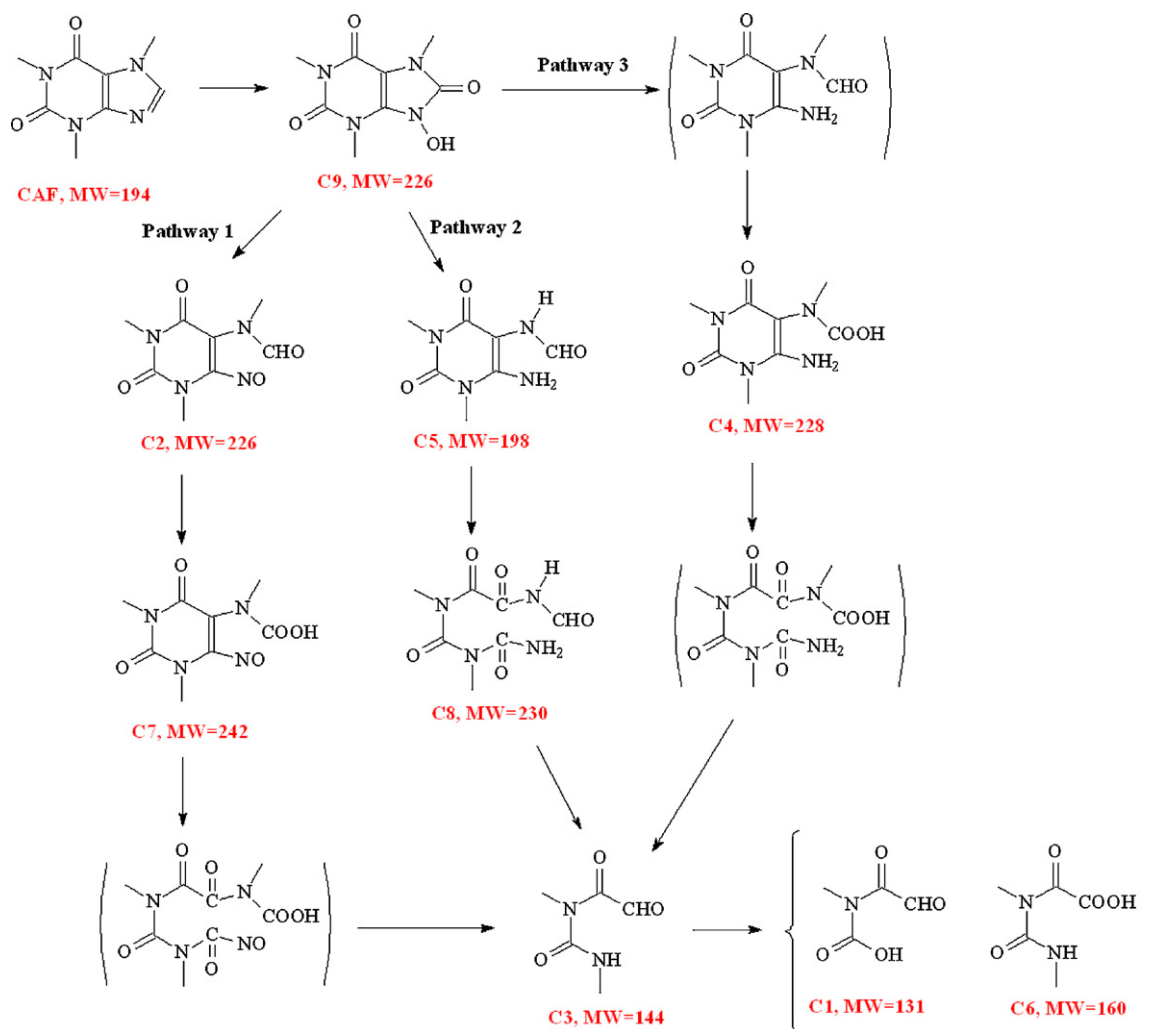


Fig. 12. Proposed degradation pathway of caffeine by Co-MCM41 activation PMS, not detected intermediates were shown in parentheses like ( ).

oxygen atoms over the CAF molecule. This is due to a ring opening, resulting from the attack of  $\text{SO}_4^{\bullet-}$  and  $\text{OH}^\bullet$  to the  $\text{N}=\text{C}$  double bond of the purine structure. Therefore, C9 may be the initial intermediate that can be identified in CAF degradation process. The compounds C2 and C7 were likely to be the succeeding products of C9 via further oxidation. C7 was a further product of C2 as the  $-\text{CHO}$  being oxidized to  $-\text{COOH}$ . This pathway was denoted as pathway 1 in this study.

In the pathway 2, the protonated form of C5 (6-amino-5-(N-formylmethylamino)-1,3-dimethyluracil) with a  $m/z$  of 199 was detected in this study, knowing as a biological metabolite of CAF [54]. C5 was a product of C9, as both the  $\text{N}-\text{CO}$  and methyl were replaced by hydrogen atom. The degraded product of C5 was C8 (detected in the positive mode). Two carbonyl groups were generated on the carbon bonding with nitrogen, when the  $\text{C}=\text{C}$  double bond was under attacked by  $\text{SO}_4^{\bullet-}$  or  $\text{OH}^\bullet$ . The generation of carbonyl groups led to the opening of the six-member ring. This intermediate was an important proof of the ring opening. In previous studies, C8 or compounds with the similar structure of C8 have never been detected, it was only reported as a proposed intermediate.

In the pathway 3, C4 was presented in the presence of the sodium adduct ( $m/z$  249) at a negative ESI/MS mode. C4 was also originated from C9 via the breakdown of the  $\text{N}-\text{CO}$  bond. However, the precursor of C4 with carbonyl was not detected in either positive or negative mode.

Among all intermediates, the C3 (at  $m/z$  142.95 in negative mode of ESI/MS) was an abundant and highly oxidized product. It can be generated from C7, C5 and C4 due to the opening of the ring when the  $\text{C}=\text{C}$  double bond was attacked by  $\text{SO}_4^{\bullet-}$  or  $\text{OH}^\bullet$ . These intermediates with  $\text{C}=\text{C}$  double bond (2nd ring in the CAF) once opened will generate the C3 as an important and abundant product (verified in this study). It should be noted that from C7, C5 and C4 to C3 is not a one-step process, some intermediates must exist in between; however, none of these has been reported or verified before. In this study, one of the critical intermediates, C8, has been identified as the first time, which makes the existence of the other two possible (as proposed in Fig. 12).

The bond  $-\text{CH}=\text{O}$  in C3 could be further oxidized to  $-\text{COOH}$ , which was detected and noted as C6 in this study (negative mode as sodiated adducts with a  $m/z$  of 180.88). In addition to C6, another possible oxidative product of C3 was also detected as noted as C1. According to the variation of intermediates structure, the proposed degradation pathway is shown in Fig. 12.

Fig. 13(A) depicts the concentration variation of CAF and degraded intermediates. The C3 and C5 were the dominant intermediates with higher concentration than the others. The accumulation of C3 suggests that it will be the final product if the initial PMS is deficient. The higher concentration of C5 implied that the proposed degradation pathway 2 was likely the main reaction. Moreover, the variations of TOC and mass balance are shown in Fig. 13(B), where the mineralization efficiency was about 13.23%

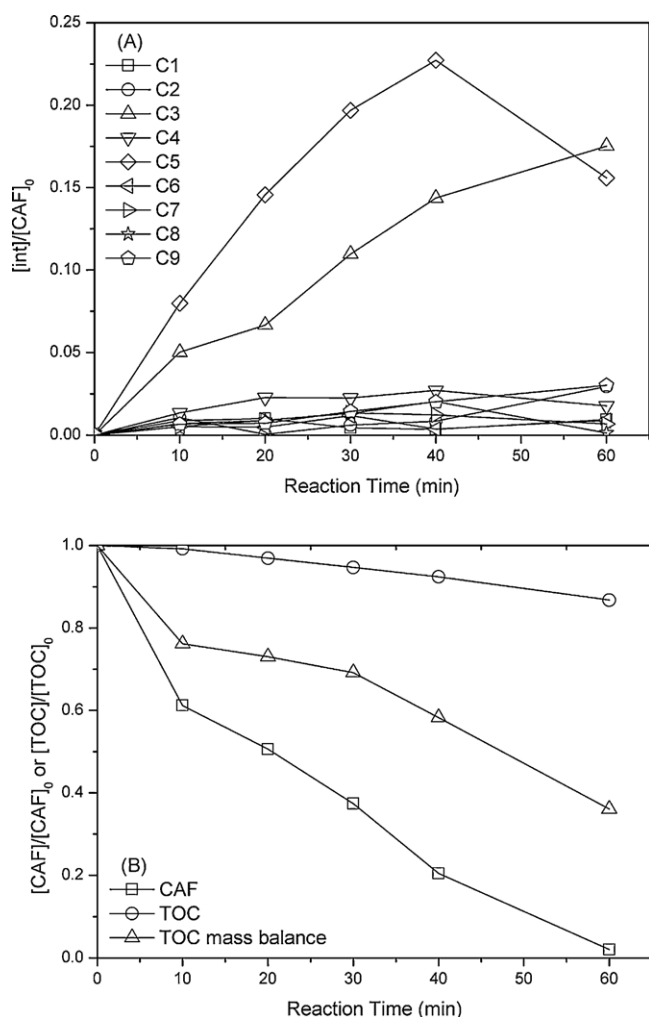


**Fig. 13.** Evolution profiles of caffeine and intermediates during the reaction of the combination of Co-MCM41 and PMS. Reaction condition: [CAF]<sub>0</sub> = 0.5 mM, [PMS]<sub>0</sub> = 10.0 mM, [catalyst] = 200 mg/L, water pH was at 7.10 with 0.1 M NaOH.

as 98.00% of CAF being decayed. As the reaction time increasing, the contribution of detected intermediate to the mass balance gradually decreased, suggesting the formation of some short-chain carboxylic acids in the solution.

#### 4. Conclusion

In summary, cobalt incorporated MCM41 was explored and justified as an efficient catalyst for activating PMS. A good degradation performance and mineralization of caffeine in aqueous solution by Co-MCM41 activated PMS process were observed. The leaching of cobalt ions in this process was insignificant because of the cobalt was incorporated into the structure of MCM41 rather than being simply attached on the surface. The heterogeneous reaction played an important role in this process, while the reaction in homogeneous phase was found minor. Both  $\text{SO}_4^{\bullet-}$  and  $\text{OH}^{\bullet}$  were believed to exist in this process, and the dominant oxidant species was  $\text{SO}_4^{\bullet-}$ . Furthermore, nine intermediates generated in this process were observed, in which 3 of them were detected for the first time. And the degradation pathway was proposed.

#### Acknowledgements

This work was carried out with the support of Hong Kong Scholars Program, a funding from the Hong Kong Polytechnic

University (G-YZ09), the National Natural Science Foundation of China (Nos. 51108030, 40903038 and 41273137), Beijing Natural Science Foundation (No. 8132033), the Specialized Research Fund for the Doctoral Program of Higher Education (No. 20100014120001), and China Post Doctoral Science Foundation (Nos. 201104060 and 2012M520006).

#### Appendix A. Supplementary data

Supplementary data associated with this article can be found, in the online version, at <http://dx.doi.org/10.1016/j.apcatb.2013.01.038>

#### References

- [1] F. Bonvin, R. Rutler, N. Chevre, J. Halder, T. Kohn, *Environmental Science and Technology* 45 (2011) 4702–4709.
- [2] J. Martin, M.D. Camacho-Munoz, J.L. Santos, I. Aparicio, E. Alonso, *Journal of Environment Management* 102 (2012) 18–25.
- [3] V. Matamoros, C.A. Arias, L.X. Nguyen, V. Salvado, H. Brix, *Chemosphere* 88 (2012) 1083–1089.
- [4] M. Lahti, A. Oikari, *Environmental Toxicology and Chemistry* 31 (2012) 1738–1744.
- [5] V. Roos, L. Gunnarsson, J. Fick, D.G.J. Larsson, C. Ruden, *Science of the Total Environment* 421 (2012) 102–110.
- [6] J. Herney-Ramirez, M.A. Vicente, L.M. Madeira, *Applied Catalysis B* 98 (2010) 10–26.
- [7] F. Qi, B.B. Xu, L. Zhao, Z.L. Chen, L.Q. Zhang, D.Z. Sun, J. Ma, *Applied Catalysis B* 121 (2012) 171–181.
- [8] T. Zhang, W.W. Li, J.P. Croue, *Applied Catalysis B* 121 (2012) 88–94.
- [9] A. Kambur, G.S. Pozan, I. Boz, *Applied Catalysis B* 115 (2012) 149–158.
- [10] M. Sturini, A. Speltini, F. Maraschi, A. Profumo, L. Pretali, E.A. Irastorza, E. Fasani, A. Albini, *Applied Catalysis B* 119 (2012) 32–39.
- [11] B.B. Xu, Z.L. Chen, F. Qi, J. Ma, F.C. Wu, *Journal of Hazardous Materials* 168 (2009) 108–114.
- [12] B.B. Xu, Z.L. Chen, F. Qi, J. Ma, F.C. Wu, *Journal of Hazardous Materials* 179 (2010) 976–982.
- [13] I.S.X. Pinto, P. Pacheco, J.V. Coelho, E. Lorencon, J.D. Ardisson, J.D. Fabris, P.P. de Souza, K.W.H. Krambrock, L.C.A. Oliveira, M.C. Pereira, *Applied Catalysis B* 119 (2012) 175–182.
- [14] P.R. Shukla, S.B. Wang, H.Q. Sun, H.M. Ang, M. Tade, *Applied Catalysis B* 100 (2010) 529–534.
- [15] Y.F. Huang, Y.H. Huang, *Journal of Hazardous Materials* 167 (2009) 418–426.
- [16] P. Shukla, H.Q. Sun, S.B. Wang, H.M. Ang, M.O. Tade, *Separation and Purification Technology* 77 (2011) 230–236.
- [17] Y.H. Guan, J. Ma, X.C. Li, J.Y. Fang, L.W. Chen, *Environmental Science and Technology* 45 (2011) 9308–9314.
- [18] S.N. Su, W.L. Guo, C.L. Yi, Y.Q. Leng, Z.M. Ma, *Ultrasonics Sonochemistry* 19 (2012) 469–474.
- [19] P. Neta, R.E. Huie, A.B. Ross, *Journal of Physical and Chemical Reference Data* 17 (1988) 1027–1284.
- [20] G.V. Buxton, C.L. Greenstock, W.P. Helman, A.B. Ross, *Journal of Physical and Chemical Reference Data* 17 (1988) 513–886.
- [21] G.P. Anipsitakis, D.D. Dionysiou, *Applied Catalysis B* 54 (2004) 155–163.
- [22] R.X. Yuan, S.N. Ramjaun, Z.H. Wang, J.S. Liu, *Journal of Hazardous Materials* 196 (2011) 173–179.
- [23] P. Nfodzo, H. Choi, *Chemical Engineering Journal* 174 (2011) 629–634.
- [24] K.H. Chan, W. Chu, *Water Research* 43 (2009) 2513–2521.
- [25] H.Q. Sun, H.Y. Tian, Y. Hardjono, C.E. Buckley, S.B. Wang, *Catalysis Today* 186 (2012) 63–68.
- [26] H.W. Liang, Y.Y. Ting, H.Q. Sun, H.M. Ang, M.O. Tade, S.B. Wang, *Journal of Colloid and Interface Science* 372 (2012) 58–62.
- [27] P. Shukla, H.Q. Sun, S.B. Wang, H.M. Ang, M.O. Tade, *Catalysis Today* 175 (2011) 380–385.
- [28] P. Shukla, S.B. Wang, K. Singh, H.M. Ang, M.O. Tade, *Applied Catalysis B* 99 (2010) 163–169.
- [29] L.E. Jacobs, L.K. Weavers, E.F. Houtz, Y.P. Chin, *Chemosphere* 86 (2012) 124–129.
- [30] F.J. Beltran, A. Aguinaco, J.F. Garcia-Araya, *Ozone Science and Engineering* 34 (2012) 3–15.
- [31] L.K.C. De Souza, J.J.R. Pardaul, J.R. Zamian, G.N. da Rocha, C.E.F. da Costa, *Journal of Thermal Analysis and Calorimetry* 106 (2011) 355–361.
- [32] R.E. Ball, J.O. Edwards, M.L. Haggett, P. Jones, *Journal of the American Chemical Society* 89 (1967) 2331–2333.
- [33] Q. Zhao, Y.H. Xu, Y.H. Li, T.S. Jiang, C.S. Li, H.B. Yin, *Applied Surface Science* 255 (2009) 9425–9429.
- [34] W.C. Zhan, G.Z. Lu, Y.L. Guo, Y. Guo, Y.S. Wang, *Journal of Rare Earths* 26 (2008) 59–65.
- [35] M. Boutros, F. Launay, A. Nowicki, T. Onfro, V. Herledan-Semmer, A. Roucoux, A. Gedeon, *Journal of Molecular Catalysis A: Chemical* 259 (2006) 91–98.
- [36] T. Somanathan, A. Pandurangan, D. Sathiyamoorthy, *Journal of Molecular Catalysis A: Chemical* 256 (2006) 193–199.

- [37] I. Zacharakis, C.G. Kontoyannis, S. Boghosian, A. Lycourghiotis, C. Kordulis, *Catalysis Today* 143 (2009) 38–44.
- [38] R. Xu, H.C. Zeng, *Chemistry of Materials* 15 (2003) 2040–2048.
- [39] Q.J. Yang, H. Choi, D.D. Dionysiou, *Applied Catalysis B* 74 (2007) 170–178.
- [40] G.A.H. Mekheimer, H.M.M. Abd-Allah, S.A.A. Mansour, *Colloids and Surfaces A* 160 (1999) 251–259.
- [41] G.P. Anipsitakis, E. Stathatos, D.D. Dionysiou, *Journal of Physical Chemistry B* 109 (2005) 13052–13055.
- [42] S. Muhammad, E. Saputra, H.Q. Sun, J.D. Izidoro, D.A. Fungaro, H.M. Ang, M.O. Tade, S.B. Wang, *RSC Advances* 2 (2012) 5645–5650.
- [43] G.L. Zhou, H.Q. Sun, S.B. Wang, H.M. Ang, M.O. Tade, *Separation and Purification Technology* 80 (2011) 626–634.
- [44] W. Zhang, H.L. Tay, S.S. Lim, Y.S. Wang, Z.Y. Zhong, R. Xu, *Applied Catalysis B* 95 (2010) 93–99.
- [45] E. Saputra, S. Muhammad, H.Q. Sun, H.M. Ang, M.O. Tade, S.B. Wang, *Catalysis Today* 190 (2012) 68–72.
- [46] J. Rivas, O. Gimeno, T. Borralho, J. Sagasti, *Desalination* 279 (2011) 115–120.
- [47] P.M. Álvarez, J. Jaramillo, F. López-Piñero, P.K. Plucinski, *Applied Catalysis B* 100 (2010) 338–345.
- [48] A.G. Trovó, T.F.S. Silva, O. Gomes Jr., A.E.H. Machado, W.B. Neto, P.S. Muller Jr., D. Daniel, *Chemosphere* 90 (2013) 170–175.
- [49] N. Klammerth, N. Miranda, S. Malato, A. Agüera, A.R. Fernández-Alba, M.I. Maldonado, J.M. Coronado, *Catalysis Today* 144 (2009) 124–130.
- [50] Y.R. Wang, W. Chu, *Journal of Hazardous Materials* 186 (2011) 1455–1461.
- [51] Y.R. Wang, W. Chu, *Water Research* 45 (2011) 3883–3889.
- [52] E. Hayon, A. Treinin, J. Wilf, *Journal of the American Chemical Society* 94 (1972) 47–57.
- [53] J.P. Telo, A. Vieira, *Journal of the Chemical Society: Perkin Transactions 2* (1997) 1755–1757.
- [54] E. Schrader, G. Klaunick, U. Jorritsma, H. Neurath, K.I. Hirsch-Ernst, G.F. Kahl, H. Foth, *Journal of Chromatography B* 726 (1999) 195–201.